The Research Council of Norway (NFR)

NORSAR

NORSAR Scientific Report No. 1-98/99

Semiannual Technical Summary

1 April – 30 September 1998

Kjeller, October 1998

7.5 Tuning the automatic data processing for the Spitsbergen array (SPITS)

Introduction

The Spitsbergen array (SPITS) usually reports a large number of detections, which can easily exceed several thousand per day. A detailed analysis shows that these detections are real seismic signals mostly caused by small sources located at close distances. These local sources are mining induced events from a coal mining area near Longyearbyen on Spitsbergen and so-called icequakes, which means active faults and fissures in the ice of nearby glaciers or stepwise movements of these glaciers (*e.g.* Górski, 1997). Because SPITS was not designed for optimized detection and analysis of such signals, they are not properly handled by the current automatic data processing and cause many erroneous results. In this study we have developed new processing recipes for SPITS that make the automatic results more reliable.

The numerous local events (Fig. 7.5.2) typically show P onsets, no well defined S onsets, and dominant Rg onsets. Because of the short epicentral distances of these events (most of them can be located within 15 km of SPITS) the travel-time difference between P and Rg onsets is only a few seconds. The current automatic processing for SPITS data has difficulty separating these onsets and locating the events, because the time windows necessary for analyzing the onsets often contain a mixture of signals with different apparent velocities (Pg, Sg, and Rg). Additionally, the array was not designed to detect local Rg phases or to estimate the slowness vector for very slow arrivals. Using the known equations to calculate the array transfer function (*e.g.* Harjes and Henger, 1973) one can estimate the design limits of an array; *e.g.*, to measure the slowness vector of an Rg phase with an apparent velocity of 1.8 km/s and a dominant frequency of about 4 Hz, an array with a minimum distance between its single sites of 0.225 km would be needed. The distances between the A-ring sites of SPITS are of this order, but not the B-ring sites (Fig. 7.5.1). To analyze these data by using only the four A-ring sites would be possible, but this would clearly decrease the stability and resolution of the slowness-vector measurements. Some of these local events are so close that the concept of a plane wave crossing an array can no longer be used, and the single sites behave as a seismic network. With these local signals, SPITS is at the edge of its resolution and the automatic f-k analysis of onsets from such events can be influenced by aliasing effects due to the side-lobes of the array transfer function.

These problems lead to many unpredictable and erroneous results for an automatic parameter extraction of SPITS detections. The most critical parameters in this context are measurements of apparent velocity and azimuth, which are used to define the phase type and are needed during the association process to define seismic events. A high error rate in f-k results leads to a high rate of erroneous or artificial events and many unassociated onsets. This problem is the main reason why SPITS onsets are not yet implemented in the Generalized Beamforming (GBF, Ringdal and Kværna, 1989) processing at NORSAR, although SPITS data would be very helpful for identifying and locating seismic events north of Fennoscandia, in the Arctic Ocean, and especially in the Barents Sea.

A New Beam Set to Improve the Detection Process

SPITS is located on Mesozoic sediments, which are about 3 to 4 km thick in this part of Spitsbergen (Winsnes, 1988). The seismic velocities in these layers are much lower than below the well known arrays in Fennoscandia, and consequently the observed apparent velocities for onsets of local events are relatively low (*e.g.,* the observed apparent velocities for local Rg phases become as small as 1.5 km/s). Therefore, the beam deployment must be expanded to lower velocities. Before beamforming, all traces are prefiltered with a Butterworth band-pass filter between 0.4 and 18.0 Hz to reduce the influence of the microseisms, which often have high amplitudes so close to the open ocean. The beam parameters (apparent velocity and azimuth) were chosen such that the whole slowness space of interest is equally covered. After beamforming, the beams are filtered with different Butterworth band-pass filters to detect the signals in the frequency range with the highest signal-to-noise ratio (SNR). Table 7.5.1 shows the parameters of the new beamset for SPITS, which contains 254 different beams.

Some beams (SG01 - SG36 and SM01 - SM36) were designed to detect the Rg onsets from local events. Identification of these numerous onsets at an early stage helps to extract detections from more "interesting" ones. Therefore the update rate for calculating the SNR was minimized to detect these high amplitude Rg phases separately from their leading Pg onsets. This also results in a increased number of detections in the coda of "normal" onsets; however, this can be handled during the following association and location process.

Because SPITS is the Norwegian array located closest to the former nuclear test sites on Novaya Zemlya, a special set of beams optimized for this source region was also implemented (SN01 - SN10).

In Fig. 7.5.4 we compare the density distribution of SNR values for detections using the old and the new processing recipes. Only Sn values smaller than 20 are shown in the figure. The data interval spans 159 days from 11 April to 16 September 1998. The original detector had a total of 118852 detections during this time period, with 113039 below SNR = 20. The new detector had a total of 179440 detections with 159289 below SNR = 20. The improvement is particularly evident for lower SNR values. Although the new beam deployment uses a higher detection threshold and no incoherent beams, the number of detected onsets is significantly increased.

A still unsolved problem at SPITS is the large number of high SNR P detections from regional events without any corresponding detection of an S phase. Without a detected S phase, these events cannot be associated and located with RONAPP (Mykkeltveit and Bungum, 1984). Fig. 7.5.3 shows seismograms observed at the 3C site SPB4 of SPITS from an earthquake located at the Knipovich Ridge northwest of Svalbard at an epicentral distance of about 3°. In addition to the original horizontal components, the rotated radial and transverse components are also shown (at the bottom). The S onset has a low SNR and the signal is particularly weak for SV energy, which should be visible on the radial and vertical components.

Just detecting this S phase on one horizontal component would not help, because the corresponding SNR on the vertical components, which has to be used for an f-k analysis, is very low and therefore the f-k results become unreliable. Additionally, at all sites of SPITS we observe spikes in the data stream, such that a detector only running on one trace will have a relatively

high false alarm rate. The best way to reduce the problem of these undetected S phases would be to install more horizontal components, so that horizontal beams could be calculated. The advantages of such beams have previously been demonstrated for other small aperture arrays like ARCESS, NORESS, and GERESS (Schweitzer, 1994).

Improving the f-k Analysis of Detected Phases

The problems discussed above influence the results from the automatic f-k analysis. We will in the following describe procedures for reducing the effect of these problems.

As mentioned above, we observe spikes which often cause false detections or disturbances of detected onsets. Most of these spikes are detected and automatically removed by the installed quality control system. However, not all spikes are detected and then they produce signal-like onsets with the pulse form of the response of the band pass filter used. The traces with the filtered spikes usually show much higher amplitudes than the undisturbed traces. Therefore, the data of all channels are checked for large amplitude deviations in the time window around the detected signal (*i.e.*, from 10 s before to 3 s after the detected onset time). If a maximum amplitude deviates more than a factor of 2.5 (smaller or larger) from the mean maximum amplitude, the data of this channel will not be used (masked) during the subsequent analysis of the detection.

Fig. 7.5.2 shows that the original amplitudes can vary by a factor of 3 between the single sites. Such amplitude variations also influence the f-k analysis. To reduce the influence of amplitude variations at the different sites, all traces are normalized to a common maximum amplitude in the time window used for the f-k analysis. However, the beam to measure the signal amplitude, dominant frequency, and onset time is calculated from non-normalized traces.

The positioning and length of the time window used for f-k analysis of the detected onset influences the f-k results and must be carefully selected. As described by Schweitzer (1994 and 1997), the optimum length of the time window can be estimated from the signal frequency band, the aperture of the array, and the largest slowness to be resolved. For SPITS the largest slowness SMAX is:

$$SMAX = \frac{1.666}{FK1}$$

when FK1 the lowest frequency used in the f-k analysis.

The time window for the f-k analysis should include the whole pulse form of the onset at all array sites. Because the onset time is given relative to the reference site of SPITS (SPA0), we need to introduce a lead time TN before the onset as the start time of the f-k analysis window. This is done to ensure that even for the arrivals with the largest slowness (smallest apparent velocity) the f-k analysis window includes the start of the signal at all array sites. For SPITS we get the relation:

$$TN = \frac{1}{2 \cdot SMAX}$$

The pulse length is initially set to 3 times the dominant period of the detected signal. For onsets detected on beams used with an apparent velocity below the local S velocity, this time length is

set to 6 times the dominant period. The f-k window length is then estimated by adding this pulse length to TN. The final f-k window length is restricted to the range between 1.5 and 5 s, which are numbers derived from manual analysis of numerous signals.

Broadband f-k analysis usually provides quite stable results. However, the detection process sometimes needs narrow band filters to detect a signal. As shown for the Matsushiro array (Schweitzer, 1997) f-k analysis results can be improved by widening the frequency range as far as possible. Therefore, a systematic search for the widest frequency range with a usable SNR was implemented.

Prior to f-k analysis in the now broader frequency range, the data are band pass filtered in a pass band slightly wider than the frequency range to be used for f-k analysis (Schweitzer, 1994). After normalizing the amplitudes, defining the smallest resolvable apparent velocity, the length of the time window, and the best frequency band, all parameters for the following f-k analysis are now set.

Although the maximum elevation difference between the single sites of SPITS is only 140 m, the corresponding travel-time differences for waves with nearly vertical incidence can be in the same order as the travel-time differences caused by the horizontal distances between the sites. The reason for this is the low seismic velocities in the sediments below SPITS. To correct for this effect during the f-k analysis, we have to know the local velocity below the array. Therefore, the best local velocities for P and S waves were estimated by comparing the f-k results for a large number of onsets with a wide range of apparent velocities after correcting with different local velocities. Assuming that the result with the highest relative f-k power is the best one for a given onset, we found that the best velocity to correct for the elevation effect is 4.75 km/s for P waves and 3 km/s for S waves. For P and S phases from local events, similar apparent velocities are observed, *i.e.*, we observe at SPITS an overlap of observable apparent velocities of regional Sn onsets and local Pg onsets, which are different from what we observe on the European continent. The slowest local Pg phases observed at regional arrays in Europe have apparent velocities between 5.5 and 6.0 km/s and observed short-period Sn phases have apparent velocities below 5.0 km/s. To resolve this ambiguity for SPITS data, all f-k analyses are done twice: once using the P phase and once the S phase local velocity to correct for the elevation effect. If the measured apparent velocity of the onset is between 4.75 and 6.0 km/s, we choose the result with the highest relative f-k power: If this was obtained using the P velocity, the phase is assumed to be a local Pg, and if this was obtained using the S velocity, the phase is assumed to be an Sn phase. If in the latter case we obtain an apparent velocity higher than the local P velocity, the phase is labeled as "Spg", to indicate that this phase is presumably an Sn, and not a local Pg.

As mentioned above, SPITS detects numerous local Rg phases which have often been misinterpreted during the automatic processing. This is primarily due to the mixture of onsets with different apparent velocities and the mentioned aliasing effect. Since an onset time estimated from the detecting beam may not be the best reference time to identify such an Rg onset, the f-k analysis is repeated for a total of six time windows. These begin TN seconds prior to the following reference times:

1) estimated onset time from the detecting beam
2) detection time from detection process
3) 0.5 s after the detection time from the detecting beam
4) 1 s earlier than the detection time from the detecting beam
5) reestimated time when the SNR reaches its threshold value
6) time when the SNR has its maximum
7) a fixed time window of +/- 1.5 s around the detection time from the detecting beam

The analysis yielding the maximum relative f-k power is preferred, excluding any for which an apparent velocity below 3 km/s (*i.e.* Rg) with a relative f-k power larger than 0.35 was found.

We will in the following compare the results from the automatic data analysis of SPITS data using the new and the old recipes. The time interval processed is the 169 day period from 11 April through 26 September 1998.

Table 7.5.2 gives the number of the different phases detected and analyzed in this time period. Except for a more detailed phase naming convention in the new recipes, the major difference is that the old recipes produce a large amount of phases with a measured apparent velocity lower than 3 km/s. These phases are called "noise" and are not further used. In the new recipes, most of these onsets are now identified as Rg. The new recipes declare as "noise" phases with an apparent velocity lower than 1.3 km/s. As mentioned, Sn phases with apparent velocities larger than the local P velocity are called Spg. They are now separated from the local Pg onsets, and can both be used to locate events. The distribution of estimated apparent velocities in Fig. 7.5.5 shows a similar result. The peak at 1 km/s disappears, and a new peak around 5 km/s represents local Pg phases, which can be used to locate these local events if a corresponding Rg (or Sg) is also observed.

The source of many of the Rg onsets (*i.e.* apparent velocities below 3 km/s) can be explained with Fig. 7.5.6, where the azimuthal distribution of these Rg phases is plotted in a rose diagram on a local map of SPITS at the position of the array. Clearly seen are distinct directions with more (longer bars) or less (shorter bars) Rg observations. To get a readable figure, the bars to the southwest in direction to the coal mine area at about 8 km distance (blue star) are truncated at about half of their lengths. We observe a strong correlation between the number of Rg phases and the azimuth at nearby glaciers (grey-blue areas). The distance to the closest glacier is about 3 km to the south.

The relative f-k power measures the coherency of the signal and is therefore a measurement of the quality of the f-k results. Fig. 7.5.7 compares the relative f-k power of body wave onsets for both sets of recipes. With the new recipes the phases with low f-k power below 0.2 are removed, and the new additional phase detections usually have high f-k power, providing well defined onsets. In Fig. 7.5.8 the relative f-k power results for the Rg phases are compared. Again, the large number of onsets with low f-k power disappear and the increased number of Rg observations for the new recipes in most cases have a relative f-k power larger than 0.35.

Conclusions

In conclusion, the new recipes for automatic analysis of SPITS data clearly increase the quality of all estimated parameters. That these new parameters are also useful as input for the

automatic location processing (RONAPP) is demonstrated with the last two figures. Fig. 7.5.9 shows a map with all events automatically located with the results from processing with the old recipes during the 169 day period from 11 April through 26 September 1998. Notice the large number of events scattered all over the map. In addition, more than 12% of the 11638 located events were located outside the borders of this map. After slight modifications of the RONAPP recipes to handle the results from the new signal processing recipes, a parallel event association and location process was also installed. Fig. 7.5.10 shows a map with 12175 located events using the new results. The decrease in the scatter is obvious, only 2% of all located events fall outside of the map and the well know seismicity pattern around and on Svalbard (*e.g.* Lindholm (1995) or Górski (1997)) is reproduced.

Starting from detection over signal analysis to the final location process, this paper shows the advantages of the new set of recipes for an automatic analysis of SPITS data. After implementing these new processing, SPITS onsets can now be included more easily in the GBF process for network phase association and event location and will most likely help to improve the event detection capability for the Arctic.

J. Schweitzer

References

Górski, M. (1997): Seismicity of the Hornsund region, Spitsbergen: icebreaks and earthquakes. Publications of the Institute of Geophysics, Polish Academy of Sciences **B-20(308)**, 76 pp.

Harjes, H.-P. and M. Henger (1973). Array-Seismologie. Zeitschrift für Geophysik **39**, 865-905.

Lindholm, C. (1995): Analysis of data recorded at the Spitsbergen array. In: NORSAR Semiannual Tech. Summ. 1 April - 30 September 1995, NORSAR Sci. Rep. **1-95/96**, Kjeller, Norway, 79-88.

Mykkeltveit, S. and Bungum, H. (1984): Processing of regional seismic events using data from small-aperture arrays. Bull. Seism. Soc. Amer. **79**, 1927-1940.

Ringdal, F. and T. Kværna (1989): A multichannel processing approach to real time network detection, phase association and threshold monitoring. Bull. Seism. Soc. Amer. **79**, 1927-1940.

Schweitzer, J. (1994). Some improvements of the detector / SigPro - system at NORSAR. In: NORSAR Semiannual Tech. Summ. 1 October 1993 - 31 March 1994, NORSAR Sci. Rep. **2-93/94**, Kjeller, Norway, 158-163.

Schweitzer, J. (1997). Recommendations for improvements in the PIDC processing of Matsushiro (MJAR) array data. In: NORSAR Semiannual Tech. Summ. 1 April - 30 September 1997, NORSAR Sci. Rep. **1-97/98**, Kjeller, Norway, 128-141.

Winsnes, T. (1988): Bedrock map of Svalbard and Jan Mayen, Norsk Polarinstitutt, **Temakart Nr. 3**.

TABLE 7.5.1. The new beamset for the SPITS array. THR is the SNR threshold used to define a detection and "all" means that the whole SPITS array (SPA0, SPA1, SPA2, SPB1, SPB2, SPB3, SPB4, and SPB5) is used to form this beam.

BEAM NAMES	VELOCITY [km/s]	AZIMUTH [°]	Filter		THR	SITES (verticals only)
			bandwidth [Hz]	order		
S001	99999.9	0.0	0.8 - 2.0	4	4.5	SPA0 SPB1 SPB2 SPB3 SPB4 SPB5
S002	99999.9	0.0	0.8 - 2.0	4	4.5	all
S003	99999.9	0.0	1.0 - 3.0	3	4.5	SPA0 SPB1 SPB2 SPB3 SPB4 SPB5
S004	99999.9	0.0	1.0 - 3.0	3	4.5	all
S005	99999.9	0.0	2.0 - 4.0	3	4.0	SPA0 SPB1 SPB2 SPB3 SPB4 SPB5
S006	99999.9	0.0	2.0 - 4.0	3	4.0	all
S007	99999.9	0.0	3.0 - 5.0	3	4.0	SPA0 SPB1 SPB2 SPB3 SPB4 SPB5
S008	99999.9	0.0	3.0 - 5.0	3	4.0	all
S009	99999.9	0.0	0.9 - 3.5	4	4.5	SPA0 SPB1 SPB2 SPB3 SPB4 SPB5
S010	99999.9	0.0	0.9 - 3.5	4	4.5	all
S011	99999.9	0.0	1.0 - 4.0	3	4.5	SPA0 SPB1 SPB2 SPB3 SPB4 SPB5
S012	99999.9	0.0	1.0 - 4.0	3	4.5	all
SA01 - SA04	10.0	0 90 180 270	1.0 - 3.0	3	4.5	SPA0 SPB1 SPB2 SPB3 SPB4 SPB5
SA05 - SA08	10.0	45 135 225 315	1.0 - 3.0	3	4.5	all
SA09 - SA12	10.0	0 90 180 270	2.5 - 4.5	3	4.0	SPA0 SPB1 SPB2 SPB3 SPB4 SPB5
SA13 - SA16	10.0	45 135 225 315	2.5 - 4.5	3	4.0	all
SA17 - SA20	10.0	0 90 180 270	4.0 - 8.0	3	4.0	SPA0 SPB1 SPB2 SPB3 SPB4 SPB5
SA21 - SA24	10.0	45 135 225 315	4.0 - 8.0	3	4.0	all
SA25 - SA28	10.0	0 90 180 270	3.0 - 6.0	3	4.0	SPA0 SPB1 SPB2 SPB3 SPB4 SPB5
SA29 - SA32	10.0	45 135 225 315	3.0 - 6.0	3	4.0	all
SB01 - SB04	7.0	0 90 180 270	1.0 - 4.0	3	4.5	SPA0 SPB1 SPB2 SPB3 SPB4 SPB5
SB05 - SB08	7.0	45 135 225 315	1.0 - 4.0	3	4.5	all
SB09 - SB12	7.0	0 90 180 270	3.0 - 6.0	3	4.0	SPA0 SPB1 SPB2 SPB3 SPB4 SPB5
SB13 - SB16	7.0	45 135 225 315	3.0 - 6.0	3	4.0	all
SB17 - SB20	7.0	0 90 180 270	5.0 - 10.0	3	4.0	SPA0 SPB1 SPB2 SPB3 SPB4 SPB5
SB21 - SB24	7.0	45 135 225 315	5.0 - 10.0	3	4.0	all
SC01 - SC04	5.0	0 90 180 270	1.0 - 4.0	3	4.5	SPA0 SPB1 SPB2 SPB3 SPB4 SPB5
SC05 - SC08	5.0	45 135 225 315	1.0 - 4.0	3	4.5	all
SC09 - SC12	5.0	0 90 180 270	3.5 - 5.5	3	4.0	SPA0 SPB1 SPB2 SPB3 SPB4 SPB5
SC13 - SC16	5.0	45 135 225 315	3.5 - 5.5	3	4.0	all
SC17 - SC20	5.0	0 90 180 270	5.0 - 10.0	3	4.0	SPA0 SPB1 SPB2 SPB3 SPB4 SPB5
SC21 - SC24	5.0	45 135 225 315	5.0 - 10.0	3	4.0	all
SC25 - SC28	5.0	0 90 180 270	8.0 - 16.0	3	4.0	SPA0 SPB1 SPB2 SPB3 SPB4 SPB5
SC29 - SC32	5.0	45 135 225 315	8.0 - 16.0	3	4.0	all
SD01 - SC08	4.0	0 45 90 135 180 225 270 315	0.9 - 3.5	4	4.5	all
SD09 - SC16	4.0	0 45 90 135 180 225 270 315	3.0 - 6.0	3	4.0	all

BEAM NAMES	VELOCITY [km/s]	AZIMUTH [°]	Filter		THR	SITES (verticals only)
			bandwidth [Hz]	order		
SD17 - SC24	4.0	0 45 90 135 180 225 270 315	4.0 - 8.0	3	4.0	all
SE01 - SE08	3.3	0 45 90 135 180 225 270 315	1.5 - 3.5	3	4.5	all
SE09 - SE16	3.3	0 45 90 135 180 225 270 315	3.0 - 6.0	3	4.0	all
SE17 - SE24	3.3	0 45 90 135 180 225 270 315	5.0 - 10.0	3	4.0	all
SF01 - SF08	2.5	0 45 90 135 180 225 270 315	1.0 - 4.0	3	4.5	all
SF09 - SF16	2.5	0 45 90 135 180 225 270 315	2.0 - 4.0	3	4.0	all
SF17 - SF24	2.5	0 45 90 135 180 225 270 315	3.0 - 5.0	3	4.0	all
SN01	8.4	97.6	2.0 - 4.0	3	3.7	all
SN02	8.4	97.6	3.0 - 5.0	3	3.7	all
SN03	8.4	97.6	4.0 - 8.0	3	3.7	all
SN04	8.4	97.6	6.0 - 12.0	3	3.7	all
SN05	8.4	97.6	8.0 - 16.0	3	3.7	all
SN06	4.7	97.6	2.0 - 4.0	3	3.7	all
SN07	4.7	97.6	3.0 - 5.0	3	3.7	all
SN08	4.7	97.6	4.0 - 8.0	3	3.7	all
SN09	4.7	97.6	6.0 - 12.0	3	3.7	all
SN10	4.7	97.6	8.0 - 16.0	3	3.7	all
SG01 - SG12	2.0	0 30 60 90 120 150 180 210 240 270 300 330	1.5 - 3.5	3	4.5	all
SG13 - SG24	2.0	0 30 60 90 120 150 180 210 240 270 300 330	2.5 - 4.5	3	4.0	all
SG25 - SG36	2.0	0 30 60 90 120 150 180 210 240 270 300 330	3.5 - 5.5	3	4.0	all
SM01 - SM12	1.7	0 30 60 90 120 150 180 210 240 270 300 330	1.0 - 3.0	3	4.5	all
SM13 - SM24	1.7	0 30 60 90 120 150 180 210 240 270 300 330	2.0 - 4.0	3	4.0	all
SM25 - SM36	1.7	0 30 60 90 120 150 180 210 240 270 300 330	3.0 - 6.0	3	4.0	all

TABLE 7.5.2. Number of onsets analyzed by the old and the new signal processing recipes during the compared time period (DOY 101 - DOY 269, 1998).

PHASE	OLD	NEW
all data	137 963	193 923
PKP	-	574
P	19 497	12 279
Pn	-	6 773
Pgn	57 333	25 360
Pg	-	38 985
S / Sn	11 691	5 208
Spg	-	4 449
Sg (Lg)	-	8 772
Rg	-	87 557
"noise"	49 442	3 965

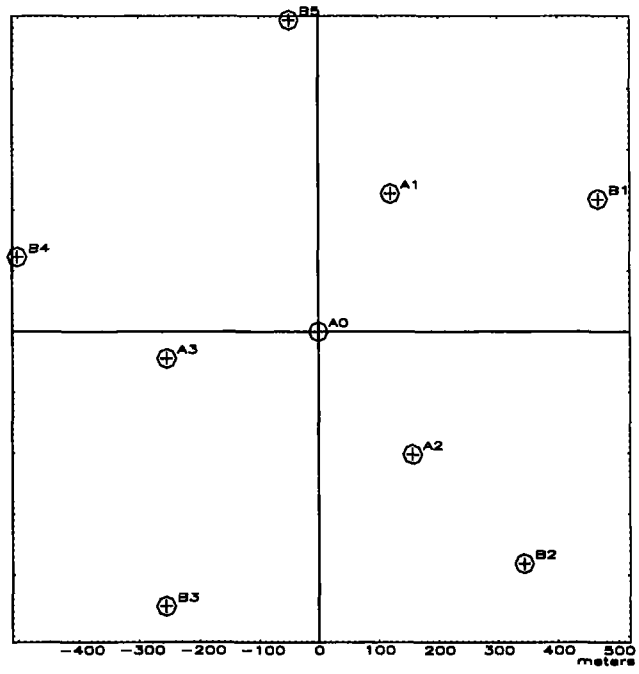

Site	X east	Y north	Z height
SPLA0.sz	0	0	323
SPLA1.sz	120	227	320
SPLA2.sz	157	-202	250
SPLA3.sz	-254	-44	339
SPLB1.sz	467	218	301
SPLB2.sz	344	-381	200
SPLB3.sz	-255	-451	234
SPLB4.sz	-501	123	340
SPLB5.sz	-49	513	295

Fig. 7.5.1. Configuration of the Spitsbergen array (SPITS). The horizontal distances are measured in [meters] with respect to the reference site SPA0 and the elevations are given in [meters] above the sea level.

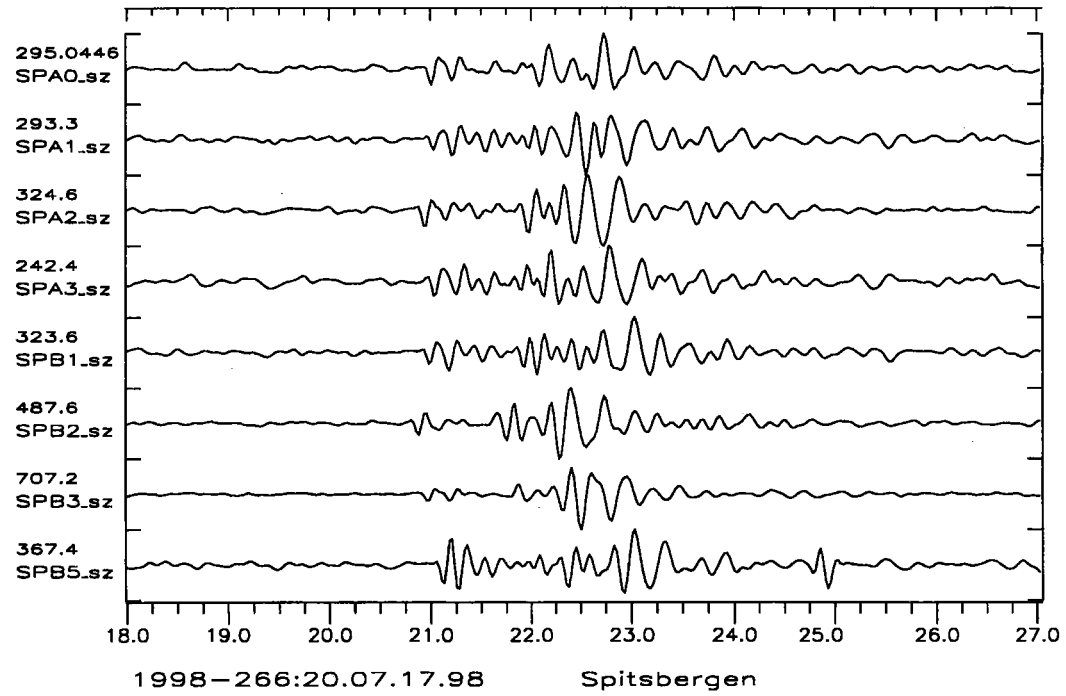

Fig. 7.5.2. Example of an "icequake" observed at SPITS and located in the glacier Gløttfjellbreen (azimuth = 141°, Δ = 4 km). Shown are band pass (3 - 8 Hz) filtered vertical seismograms.

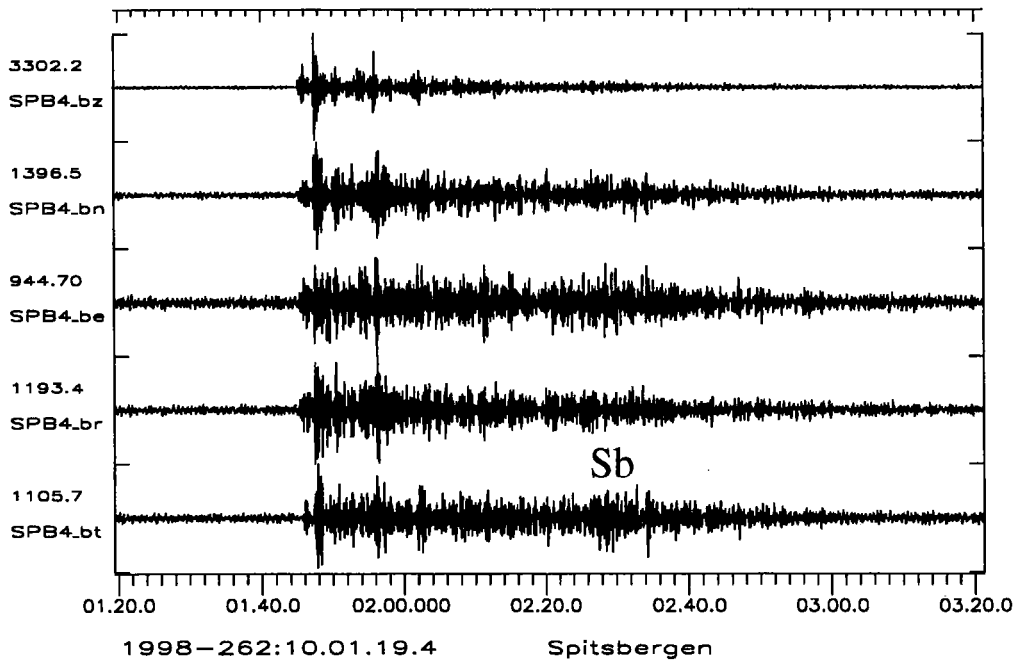

Fig. 7.5.3. Seismograms of a regional event observed with the broadband 3C site SPB4. Note the increased SNR for the Sb onsets on the transverse component (SPB4_bt). The data were band pass filtered (3 - 6 Hz); the azimuth to rotate the horizontals was 312°.

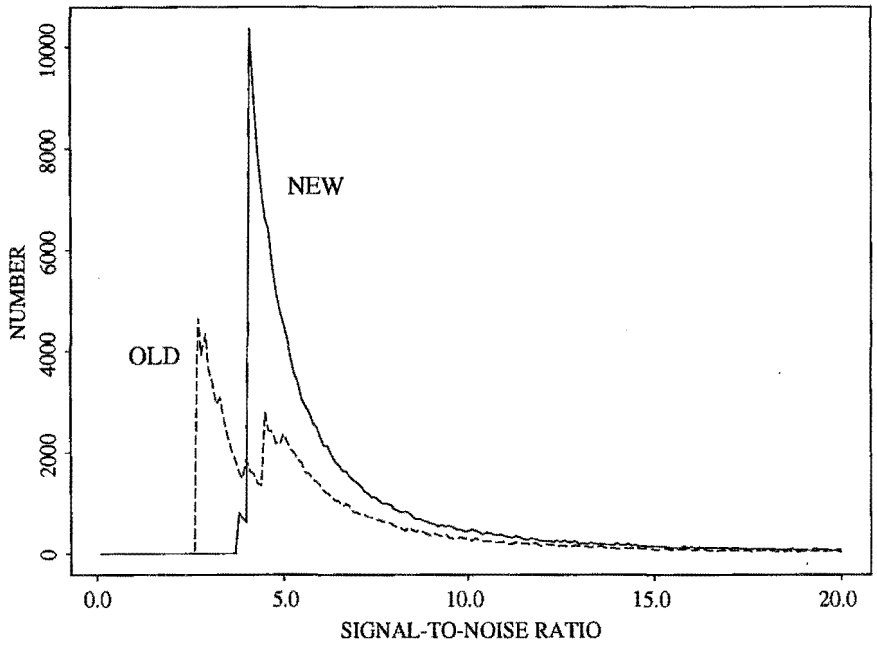

Fig. 7.5.4. Distribution of observed SNR values (SNR < 20) for the old (broken line) and the new SPITS beam deployment.

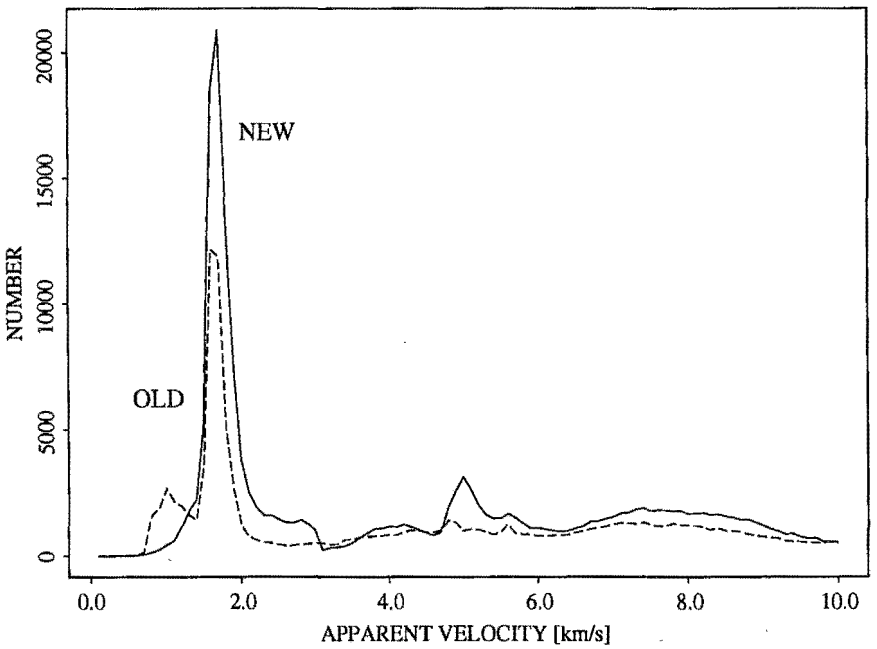

Fig. 7.5.5. Distribution of observed apparent velocities for local and regional phases for the old (broken line) and new SPITS analysis recipes.

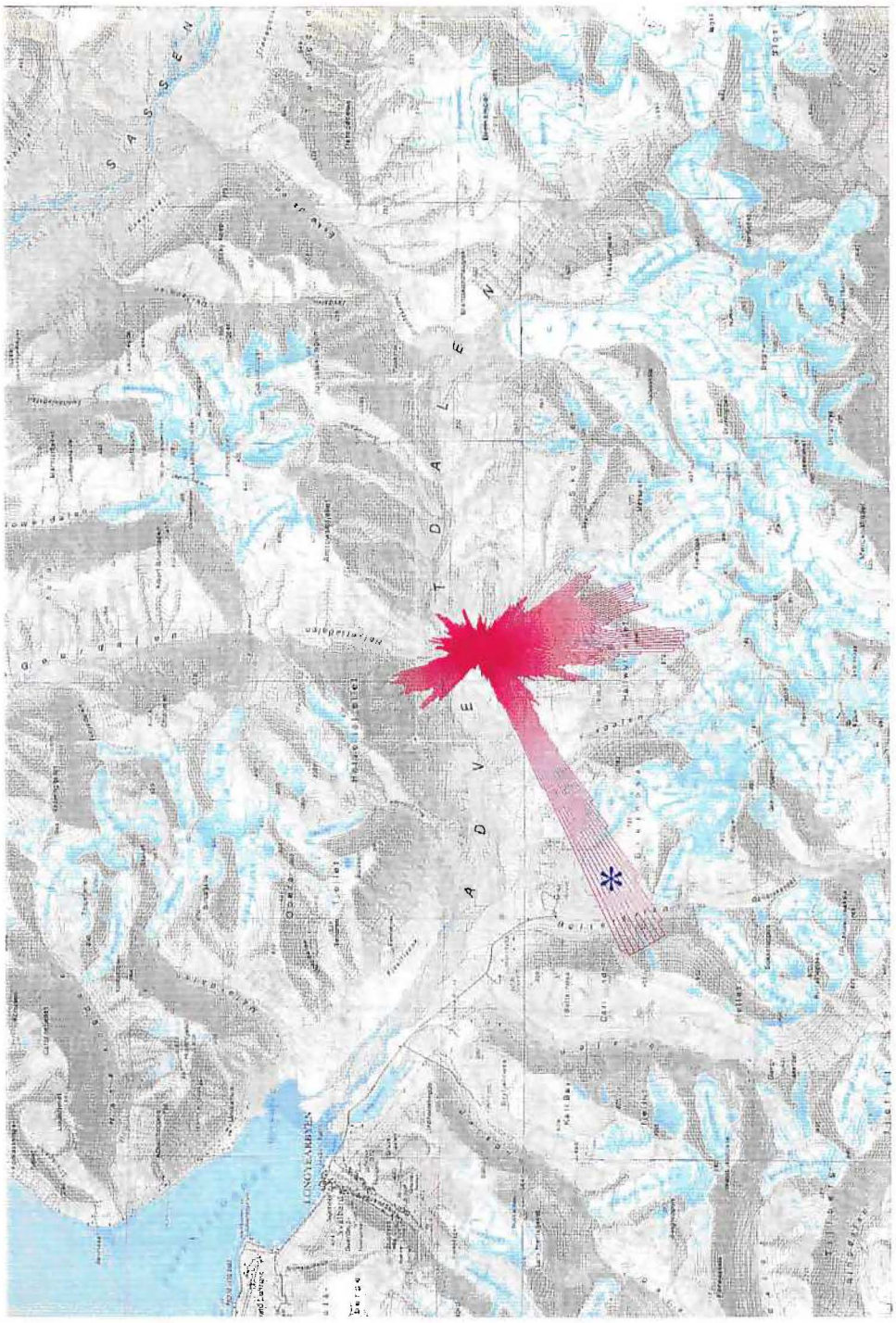

Fig. 7.5.6. Map with the area around SPITS and a rose diagram for 90228 observed local phases (apparent velocity < 3 km/s, DOY 101 to DOY 269, 1998) to show the relative azimuth distribution of these onsets. The center of the rose diagram is plotted at the center of the array. The graph for the large amount of phase observations from mining induced events (blue star) in the southwest direction was truncated at about half of its length. Note: the shorter the distance to a glacier (grey areas), the larger the number of observed Rg phases. The scale of the map is approximately 1 : 220 500.

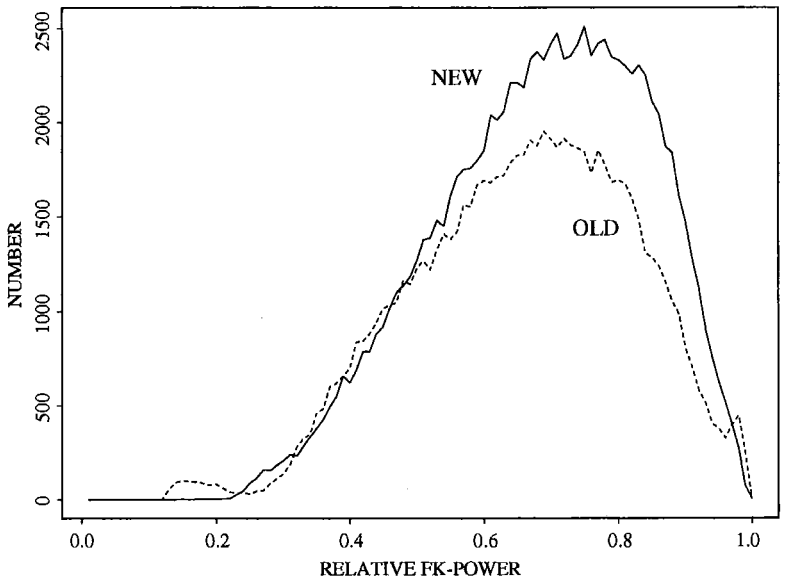

Fig. 7.5.7. Distribution of relative f-k power results for the old (broken line) and the new recipes for onsets with an apparent velocity > 3.0 km/s.

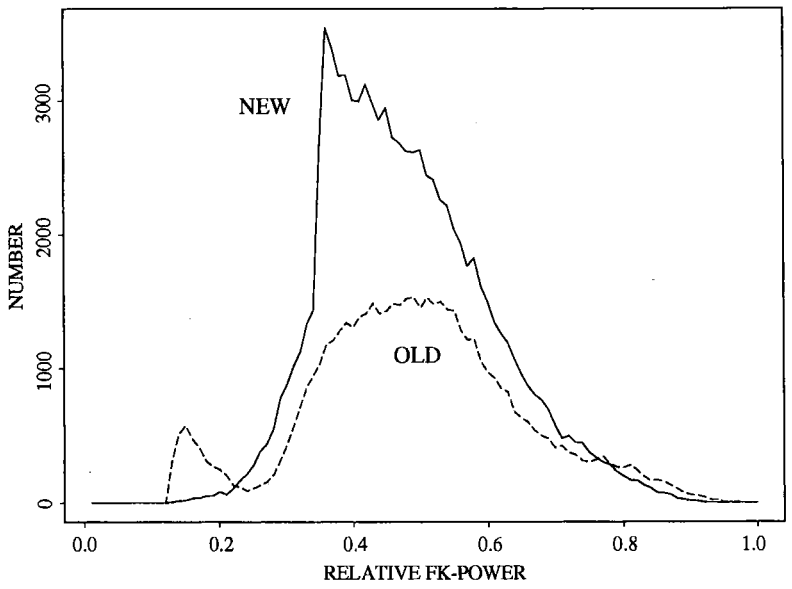

Fig. 7.5.8. Distribution of relative f-k power results for the old (broken line) and the new recipes for onsets with an apparent velocity <= 3.0 km/s.

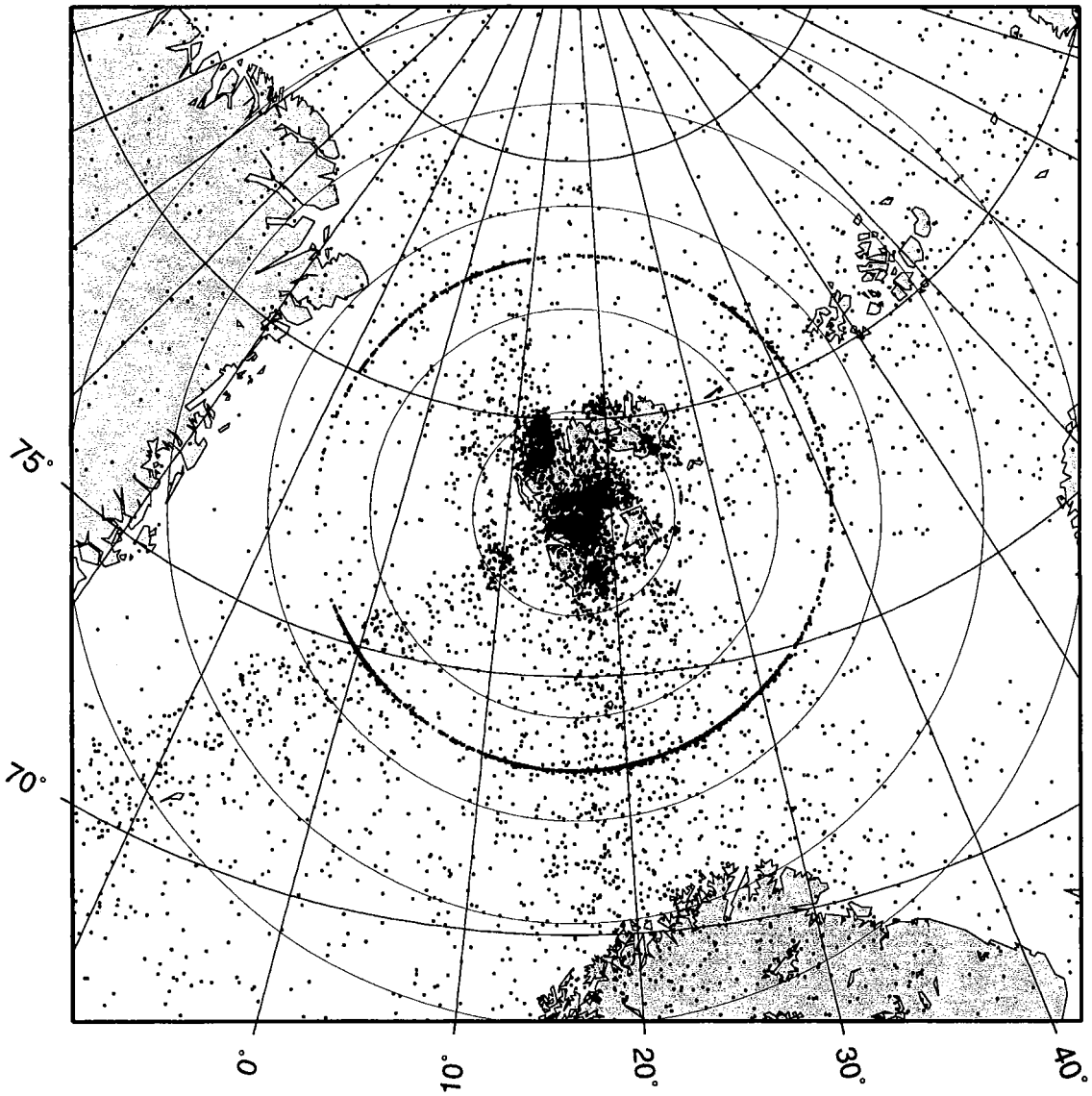

Fig. 7.5.9. SPITS single array located events using the old recipes during the 169 day period from 11 April through 26 September 1998. From the altogether 11 638 located events more than 12% were located outside this map. The circles around SPITS are at 2°, 4°, 6°, 8°, and 10° epicentral distances. The circle of events at about 5° is an artifact of an error in the old recipes.

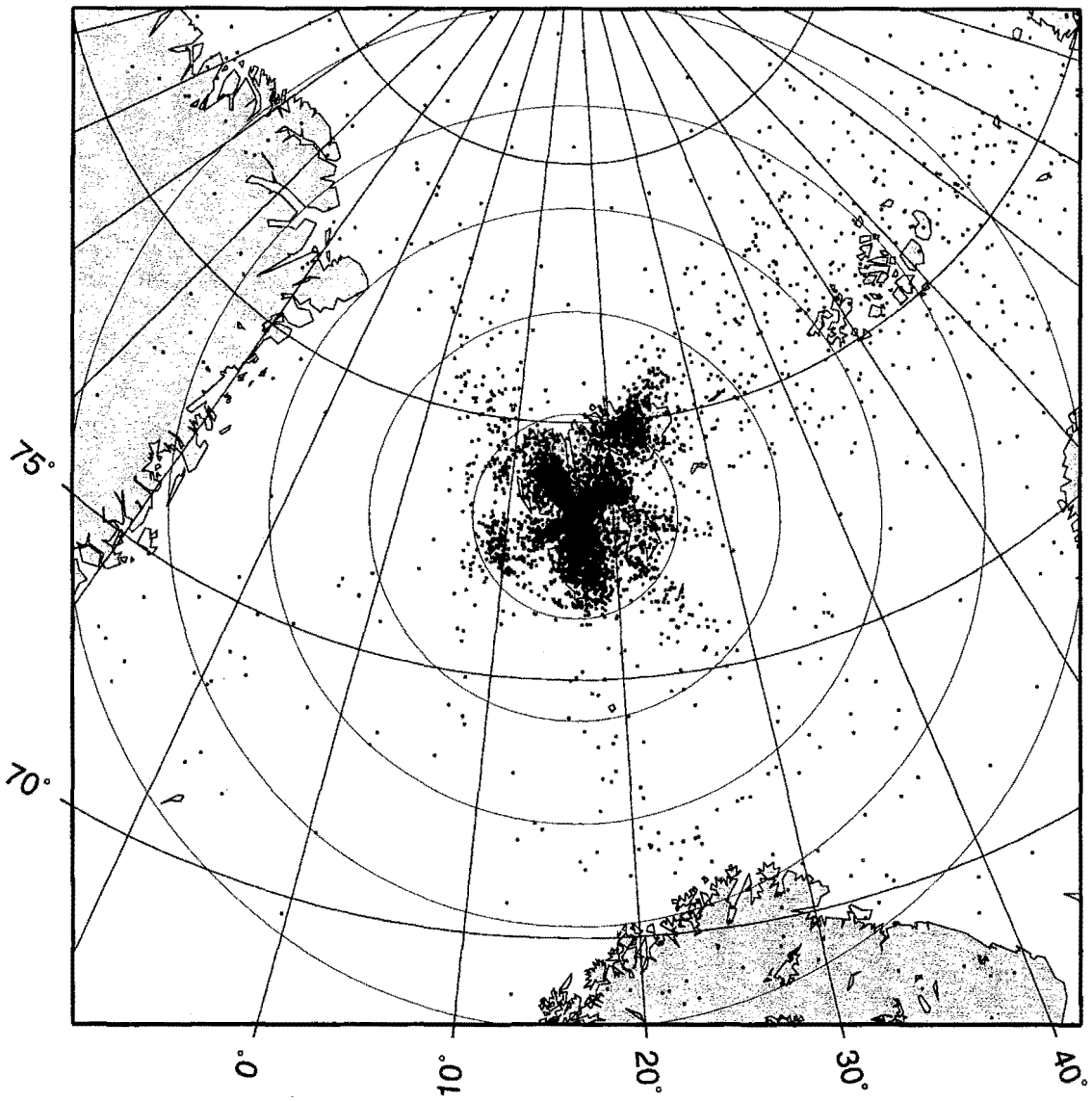

Fig. 7.5.10. SPITS single array located events using the new recipes during the 169 day period from 11 April through 26 September 1998. From the altogether 12 175 located events less than 2% were located outside this map. The circles around SPITS are at 2°, 4°, 6°, 8°, and 10° epicentral distances.